Title	Phosphorylation of myosin II regulatory light chain controls its accumulation, not that of actin, at the contractile ring in HeLa cells
Author(s)	Kondo, Tomo; Itakura, Shiho; Hamao, Kozue; Hosoya, Hiroshi
Citation	Experimental Cell Research , 318 (8) : 915 - 924
Issue Date	2012
DOI	10.1016/j.bbrc.2011.11.151
Self DOI	
URL	https://ir.lib.hiroshima-u.ac.jp/00034807
Right	(c) 2012 Elsevier Inc. All rights reserved.
Relation	

Phosphorylation of myosin II regulatory light chain controls its accumulation, not that of actin, at the contractile ring in HeLa cells

Tomo Kondo, Shiho Itakura, Kozue Hamao, and Hiroshi Hosoya*

Department of Biological Science, Graduate School of Science, Hiroshima University, Higashi-Hiroshima 739-8526, Japan

*Corresponding author: Hiroshi Hosoya

Department of Biological Science, Graduate School of Science, Hiroshima University, Higashi-Hiroshima 739-8526, Japan

Telephone: +81 82 424 7445; Fax: +81 82 424 0734

E-mail: hhosoya@hiroshima-u.ac.jp

Abbreviations

MRLC, myosin II regulatory light chain; MHC, myosin II heavy chain; F-actin, filamentous actin; CR, contractile ring; EGFP, enhanced green fluorescent protein; DAPI, 4′, 6-diamidine-2-phenylindole

Abstract

During cytokinesis in eukaryotic cells, an actomyosin-based contractile ring (CR) is assembled along the equator of the cell. Myosin II ATPase activity is stimulated by the phosphorylation of the myosin II regulatory light chain (MRLC) *in vitro*, and phosphorylated MRLC localizes at the CR in various types of cells. Previous studies have determined that phosphorylated MRLC plays an important role in CR furrowing. However, the role of phosphorylated MRLC in CR assembly remains unknown. Here, we have used confocal microscopy to observe dividing HeLa cells expressing fluorescent protein-tagged MRLC mutants and actin during CR assembly near the cortex. Di-phosphomimic MRLC accumulated at the cell equator earlier than non-phosphorylatable MRLC and actin. Interestingly, perturbation of myosin II activity by non-phosphorylatable MRLC expression or treatment with blebbistatin, a myosin II inhibitor, did not alter the time of actin accumulation at the cell equator. Furthermore, inhibition of actin polymerization by treatment with latrunculin A had no effect on MRLC accumulation at the cell equator. Taken together, these data suggest that phosphorylated MRLC temporally controls its own accumulation, but not that of actin, in cultured mammalian cells.

Keywords

myosin II regulatory light chain; actin; contractile ring; cytokinesis; phosphorylation

Introduction

The contractile ring (CR), which mainly consists of filamentous actin (F-actin) and myosin II, is formed at the equator of a cell. During cytokinesis in eukaryotic cells, the CR undergoes constriction to form a cleavage furrow. A pivotal study has shown that the furrowing occurs between centrosomes linked by mitotic spindles [1], suggesting that a signal from the mitotic apparatus determines the position of the cleavage furrow. It was subsequently revealed that the small GTPase Rho is the positional cue for the CR assembly at the cell equator [2, 3], and a midzone-localizing complex containing MKLP1, MgcRacGAP, and ECT2 is required for Rho activation during cytokinesis [4-7]. Although recent advances in functional genomics and proteomics have aided in understanding the molecular requirements of cytokinesis in eukaryotic cells [8, 9], it remains unclear how cytokinetic proteins such as F-actin and myosin II cooperate in CR assembly and constriction.

Myosin II, which is composed of three distinct types of subunits [heavy chain (MHC), essential light chain, and regulatory light chain (MRLC)], has been shown to be essential for invagination of the cleavage furrow in various cell lines [10-13]. Phosphorylation of MRLC at Ser19 (monophosphorylation) and at Thr18 and Ser19 (diphosphorylation) causes myosin II activation and the assembly of bipolar filaments *in vitro* [14, 15]. Phosphorylated and nonphosphorylated MRLC localize to the CR during cytokinesis in mammalian cells [16-21]. Our recent studies have shown that the phosphorylation of MRLC controls the dynamics of myosin II and actin at the CR, resulting in the proper speed of furrow ingression [22, 23]. In combination, these data

indicate that phosphorylated MRLC plays an important role in CR constriction in mammalian cells. However, its role in CR assembly remains unknown.

In this study, to clarify the role of phosphorylated MRLC in CR assembly, we observed equatorial MRLC and actin accumulation by using fluorescent protein-tagged phosphomimic (AD- and DD-) or non-phosphorylatable (AA-) MRLC and actin during cytokinesis in dividing HeLa cells. Di-phosphomimic MRLC (DD-MRLC) accumulated at the cell equator earlier than non-phosphorylatable MRLC (AA-MRLC) and actin. Perturbation of myosin II activity had no effect on the time of actin accumulation at the equatorial region. Furthermore, the time of MRLC accumulation was not altered by inhibition of actin polymerization. Taken together, these data suggest that the phosphorylation of MRLC regulates its own accumulation, but not that of actin, at the CR during cytokinesis in mammalian cells.

Materials and Methods

Reagents and chemicals

Mouse anti-MRLC antibody (E-4) and rabbit Living Colors A.v. Peptide Antibody were obtained from Santa Cruz Biotechnology (Santa Cruz, CA, USA) and Clontech Laboratories (Palo Alto, CA, USA), respectively. S-(–)-Blebbistatin and latrunculin A were obtained from Toronto Research Chemicals (Ontario, Canada) and Wako Pure Chemical Industries (Osaka, Japan), respectively. Rabbit anti-MHC antibody was a kind gift from Dr. K. Fujiwara (University of Rochester, Rochester, NY, USA).

Plasmid construction

The pmCherry vector and p-enhanced green fluorescent protein (EGFP)-actin were obtained from Clontech Laboratories. cDNA encoding AA/AD/DD-MRLC, in which Thr18 and Ser19 are each replaced by Ala and/or Thr [18], were inserted into pmCherry-N1. The construction of pmCherry-wild type (Wt)-MRLC or actin have been previously described [23].

Cell culture and plasmid transfection

HeLa cells (RCB0007) were obtained from the RIKEN Cell Bank (Tsukuba, Japan). The cells were cultured as previously described [23]. Transfection of plasmids was performed using Lipofectamine (Invitrogen, Carlsbad, CA, USA), according to the manufacturer's instructions.

Immunoprecipitation and western blotting

HeLa cells expressing mCherry-MRLCs, EGFP-DD-MRLC, or mCherry were collected with a rubber policeman in RIPA buffer [50 mM Tris-HCl (pH 7.5), 150 mM NaCl, 0.1% SDS, 1% Nonidet P-40, 0.5% deoxycholate, 1 mM EGTA, 1 mM PMSF, 1 μg/mL pepstatin A, and 10 mM $MgCl_2$]. The mixture was sonicated twice on ice with a Branson Sonifier 450 at 10-s pulses (60% duty cycle) at a setting of 3, and centrifuged at 15,100 ×*g* for 30 min at 4°C, and the supernatant (lysate) was collected. For immunoprecipitation, the lysate was incubated with Living Colors A.v. Peptide Antibody (1 μg) for 1 h at 4°C, and then gently agitated with Protein G Sepharose (GE Healthcare Japan, Tokyo, Japan) for 1 h at 4°C. The beads were collected by centrifugation (700 ×*g*), washed three times with RIPA buffer, and then added to SDS sample buffer. The samples were subjected to SDS-PAGE using a gradient gel (MULTIGEL II Mini 4/20; Cosmo Bio, Tokyo, Japan) and transferred to Immobilon-PSQ transfer membranes (pore size, 0.2 μm; Millipore, Billerica, MA, USA). The membranes were incubated with anti-MHC antibody (1:100) or anti-MRLC antibody (1:100) for 1 h at room temperature, and were then incubated with alkaline phosphatase-conjugated secondary antibodies (1:5,000) (Promega KK, Tokyo, Japan) for 1 h at room temperature. The blots were developed with 0.2 mg/mL nitroblue tetrazolium and 0.1 mg/mL 5-bromo-4-chloro-3-indolyl phosphate (Nacalai Tesque, Kyoto, Japan).

Indirect immunofluorescence

HeLa cells were transfected with pmCherry-MRLC and pEGFP-actin and fixed with 3.7% formaldehyde. After washing with PBS [23], the cells were mounted on a microscope slide with a drop of FluoroGuard (Bio-Rad Laboratories, Hercules, CA, USA) containing 0.5 μg/mL 4′,6-diamidine-2-phenylindole dihydrochloride (DAPI). To investigate the effect of actin polymerization, HeLa cells were treated with latrunculin A (100 nM) or DMSO for 10 or 30 min at 37°C. The cells were stained using TRITC-phalloidin (Sigma-Aldrich, St. Louis, MO, USA) for F-actin analysis as previously described [23]. Images were obtained using a FV1000-D confocal laser scanning microscope (Olympus, Tokyo, Japan) with a UPLSAPO 100× NA 1.4 oil immersion lens (Olympus). Images were processed using FluoView software (Olympus) and Adobe Photoshop.

Live cell imaging

To investigate the inhibition of CR furrowing by blebbistatin, cells were treated with 1 or 25 μM blebbistatin or DMSO for 2 h, and images were obtained using a FV1000-D microscope with a UPLSAPO 20× NA 0.75 dry lens (Olympus) and a 559-nm laser to avoid phototoxicity and photoinactivation of blebbistatin [24, 25]. To obtain images of fluorescent protein-tagged MRLCs and actin during CR assembly, we observed the area near the bottom of the cells as 1-μm step z-series using the FV1000-D microscope with

a UPLSAPO 100× (NA, 1.4) oil immersion lens. To observe CR assembly in the presence of blebbistatin, cells in the anaphase were treated with 25 μM blebbistatin or DMSO, and images were obtained. The diameter of the CR was measured using FluoView software. For observation of cells in the presence of latrunculin A, cells in the metaphase were treated with 100 nM latrunculin A or DMSO and observed for 6 h. Fluorescence measurements and image processing were performed with FluoView software and Adobe Photoshop, respectively. The accumulation time of MRLC or actin was defined as the period (min) from the onset of anaphase to the time when the relative fluorescence intensity value at the cell equator exceeded 1.05. Statistical analysis was performed using the Student's *t*-test and the Pearson's correlation test. We confirmed that irradiation of the laser did not affect the progress of cytokinesis, including the speed of CR furrowing (data not shown).

Results

Characterization of mCherry-tagged MRLC mutants

To characterize the four mCherry-tagged MRLC mutant variants (Wt/AA/AD/DD-MRLC), we examined their physical accessibility to MHC in cells by immunoprecipitation using Living Colors A.v. Peptide Antibody. Endogenous MHC was coimmunoprecipitated with mCherry-tagged MRLC mutants from HeLa cell lysates (Fig. 1A). This was in agreement with the previous result obtained with EGFP-tagged MRLC mutants [26]. We also found that although MRLC-mCherry was immunoprecipitated in equal amounts, MHC was coprecipitated in smaller amounts from the lysate of DD-MRLC than that of Wt-, AA-, or AD-MRLC (Fig. 1A). EGFP-tagged MRLC has been shown to have the same turnover rate on MHC IIA in stress fibers and CR [23], suggesting that mCherry-tagged MRLC mutants also bind to the MHC and localize at the contractile apparatus such as the stress fibers or the CR in cells. Next, we observed the subcellular localization of DD-MRLC-mCherry as a representative of MRLC mutants. DD-MRLC-mCherry was colocalized with EGFP-actin in the interphasic (Fig. 1B, upper) and mitotic cells (Fig. 1B, lower). These data indicate that mCherry-tagged MRLC mutants can act as a myosin II subunit in cells, similar to EGFP-tagged mutants.

Phosphorylated MRLC accumulated at the cell equator earlier than nonphosphorylated MRLC

To determine whether the phosphorylation of MRLC regulates its accumulation at the

cell equator, we used confocal microscopy to observe the region near the bottom of the cortex in the dividing cells expressing AA- or DD-MRLC-mCherry (Fig. 2A). The time of MRLC accumulation at the cell equator had no correlation with its expression level (Fig. 2B). AA-MRLC was recruited 4.6 ± 0.4 min after the onset of anaphase, whereas DD-MRLC accumulated at 2.7 ± 0.3 min (Fig. 2C). These data indicate that the phosphorylation of MRLC accelerated its accumulation at the equatorial region of cells.

MRLC accumulated at the cell equator before actin

To examine whether phosphorylated MRLC controls CR assembly, each mCherry-tagged MRLC mutant was coexpressed with EGFP-actin in HeLa cells (Fig. 3A and 3D). The time of MRLC accumulation at the cell equator had no correlation with the EGFP-actin expression level (Fig. 3B) or MRLC itself (Fig. S1A). As shown in Figure 3C, the time of AA-MRLC-mCherry accumulation (5.0 ± 0.7 min after the onset of anaphase) at the cell equator of cells coexpressing EGFP-actin was significantly delayed compared with that of DD-MRLC-mCherry (3.0 ± 0.5 min), which was consistent with the results obtained in Figure 2. The time of EGFP-actin accumulation at the equator in the cells coexpressing each mCherry-tagged MRLC mutant did not correlate with the MRLC mutant expression levels (Fig. 3E) or with EGFP-actin itself (Fig. S1B). Interestingly, the expression of each MRLC mutant did not affect the time of EGFP-actin accumulation at the equator (Fig. 3F), suggesting that actin accumulation at the equator was independent of MRLC and its phosphorylation state. The differences in the accumulation time between MRLC and actin in the cells expressing Wt-, AD-, and

DD-MRLC were 0.7–1.7 min, whereas the differences in the cells expressing AA-MRLC was just 0.1 min (Fig. 3G). These data indicate that the time of actin accumulation at the cell equator was independent of MRLC, and MRLC accumulated at the cell equator earlier than actin in HeLa cells.

Myosin II ATPase activity was not required for actin accumulation at the cell equator

Next, we determined whether the accumulation of actin at the cell equator was independent of myosin II ATPase activity. Treatment with blebbistatin (25 μM), a myosin II inhibitor, significantly delayed the speed of CR contraction, but did not inhibit the completion of CR furrowing (Fig. 4A). These data suggest that treatment with blebbistatin (25 μM) was optimal to mimic the phenotype of AA-MRLC-expressing cells that only exhibit a delay in CR furrowing [22]. Cells expressing mCherry-actin were treated with blebbistatin, and then, observed (Fig. 4B). Accumulation of mCherry-actin at the cell equator did not correlate with its expression level (Fig. 4C), and blebbistatin did not alter the time of actin accumulation (Fig. 4D). These data indicate that myosin II ATPase activity was not crucial for actin accumulation at the cell equator.

MRLC accumulation at the cell equator was independent of actin accumulation

To further investigate the interaction between MRLC and actin during CR assembly, we observed cells treated with 100 nM latrunculin A, an inhibitor of actin polymerization.

Accumulation of F-actin at the equator was disrupted by latrunculin A (Fig. 5A). We further observed Wt-MRLC-mCherry accumulation in cells treated with 100 nM latrunculin A (Fig. 5B). The time of Wt-MRLC-mCherry accumulation was unaffected by its expression level (Fig. 5C). As shown in Figure 5D, latrunculin A had no effect on Wt-MRLC accumulation at the cell equator. These data suggest that MRLC accumulation at the cell equator was independent of actin accumulation.

Discussion

Our previous living cell-imaging studies revealed that both the phosphomimic and non-phosphorylatable forms of EGFP-MRLC were recruited to the equator [21]. The data obtained using mCherry-MRLCs supported these results, suggesting that phosphorylation of MRLC is not essential for recruitment of MRLC to the equator. In this study, the data obtained using a highly sensitive confocal microscope indicated that the non-phosphorylatable MRLC accumulated at the equator later than the phosphomimic MRLC did. Further, phosphomimic mutants of MRLC and blebbistatin treatment did not affect the timing of actin accumulation at the equator. These data suggest that myosin II activity is not required for recruitment of actin at the equator during cytokinesis.

The accumulation of MHC and actin at the cell equator has been observed in fixed budding yeast [27] and *Xenopus* eggs [28], and in living fission yeast [29] and cultured animal cells [30]. These studies concluded that equatorial MHC accumulation precedes actin accumulation. In fixed *Drosophila* S2 cells stably expressing MRLC, enrichment of MRLC at the cell equator was also observed earlier than that of F-actin. In these studies, however, real-time imaging of the accumulation of MHC and/or MRLC in the cells coexpressing actin was not performed. As such, we performed real-time imaging of both MHC/MRLC and actin at the equatorial cortex within the same system. Here, our real-time imaging studies using confocal microscope revealed that MRLC accumulation at the cell equator occurred earlier than actin accumulation in cultured mammalian cells co-expressing MRLC and actin. These data show that equatorial

accumulation of MHC/MRLC before actin is a fundamental mechanism of CR assembly in various types of eukaryotic cells.

An important issue is the cellular mechanism by which MHC/MRLC is recruited to the cell equator before actin. One potential regulator for assembling proteins such as actin and myosin II at the CR is Mid1/anillin in eukaryotes [31-35]. According to one of the two present models in *Schizosaccharomyces pombe*, Mid1 recruits MHC, an IQ-motif-containing GTPase activating protein, formin, and Cdc15 to the equator, and then F-actin emanated from a formin(s), forms the CR [36, 37]. On the contrary, a Mid1-independent model for CR assembly has also been proposed [32, 38]. In animal cells, MHC was recruited to the cell cortex in anillin-depleted cultured *Drosophila* Kc167 and mammalian cells [39, 40], although anillin has been reported to be a MHC- or MRLC-interacting protein [39]. Thus, the precise role of Mid1/anillin in CR assembly is highly controversial.

Another candidate as an essential protein for CR assembly is the actin/MHC-interacting protein septin [41-44]. MHC accumulation at the cell equator was not observed in the septin mutant *Saccharomyces cerevisiae* strain [27]. Although the transduction of a truncated MHC coiled-coil domain into the CHO-K1 cells inhibited the interaction between mammalian septin SEPT2 and MHC-IIA, initial accumulation of MHC-IIA at the cell equator was not altered, even in cells transfected with the domain [43], suggesting that factor(s) other than septin are required for the recruitment of MHC to the equator. Thus, the role of septin in the recruitment of MHC/MRLC to the cell equator is also controversial.

To date, there are several hypotheses, which are not mutually exclusive, of how MHC/MRLC is accumulated at the equator, such as the cortical flow hypothesis [45, 46]. Although this hypothesis has been supported by the imaging of membrane-bound beads [47], GFP-MHC [48], and myosin II itself [49], recent observations with total internal reflection fluorescence microscopy have revealed that MHC is recruited to the equator through a cortical flow-independent mechanism [30, 50]. Uyeda et al. indicated that a conformational change in actin subunits promotes the binding of myosin II [51]. Interestingly, local tension at the cell equator has been reported to increase after cell elongation to the poles [52]. Such tension at the cell equator will cause a conformational change in cortical actin and induce myosin II accumulation at the cell equator. Thus, we propose a mechanism for equatorial myosin II accumulation (Fig. 6). As shown in Figures 2 and 3, phosphorylated MRLC preferentially accumulates at the cell equator before the onset of anaphase (Fig. 6a and 6b), although its mechanism has not been elucidated. Accumulated MRLC causes an increase of cortical tension, because of the interaction with the preexisting F-actin beneath the cell membrane at the cell equator (Fig. 6c). Subsequently, more MRLC accumulates at the equator (Fig. 6d). Then, actin accumulates more effectively at the cell equator (Fig. 6e), which is followed by CR constriction.

Our recent study showed that diphosphorylated MRLC localized to the midzone independently of MHC during cytokinesis in various mammalian cultured cells [53]. Naqvi et al. reported that MRLC (cdc4p and Rlc1p) localized to the cell equator independent of MHC (Myo2p) in *Schizosaccharomyces pombe* [54, 55]. These results

suggest that a subpopulation of MRLC works without MHC. Future studies are required for additional imaging and biochemical analysis to elucidate the role of MHC-unbound MRLC and/or MRLC-unbound MHC in cytokinesis.

Acknowledgements

We thank Dr. K. Kamijo (Tohoku University, Miyagi, Japan) for providing Wt-MRLC-mCherry and mCherry-actin plasmids; Dr. K. Fujiwara (University of Rochester, Rochester, NY, USA) for providing anti-MHC antibody; and Dr. TQ. Uyeda (National Institute of Advanced Industrial Science and Technology, Ibaraki, Japan) for critically reviewing the manuscript and offering helpful comments. This work was supported by research grants for research fellow of the Japan Society for Promotion of Science to T.K., and from the Ministry of Education, Culture, Sports, Science and Technology in Japan to H.H.

References

[1] R. Rappaport, Experiments concerning the cleavage stimulus in sand dollar eggs., J Exp Zool 148 (1961) 81-89.

[2] K. Kishi, T. Sasaki, S. Kuroda, T. Itoh, Y. Takai, Regulation of cytoplasmic division of Xenopus embryo by rho p21 and its inhibitory GDP/GTP exchange protein (rho GDI), J Cell Biol 120 (1993) 1187-1195.

[3] I. Mabuchi, Y. Hamaguchi, H. Fujimoto, N. Morii, M. Mishima, S. Narumiya, A rho-like protein is involved in the organisation of the contractile ring in dividing sand dollar eggs, Zygote 1 (1993) 325-331.

[4] O. Yüce, A. Piekny, M. Glotzer, An ECT2-centralspindlin complex regulates the localization and function of RhoA., J Cell Biol 170 (2005) 571-582.

[5] W.M. Zhao, G. Fang, MgcRacGAP controls the assembly of the contractile ring and the initiation of cytokinesis., Proc Natl Acad Sci U S A 102 (2005) 13158-13163.

[6] K. Kamijo, N. Ohara, M. Abe, T. Uchimura, H. Hosoya, J.S. Lee, T. Miki, Dissecting the role of Rho-mediated signaling in contractile ring formation., Mol Biol Cell 17 (2006) 43-55.

[7] Y. Nishimura, S. Yonemura, Centralspindlin regulates ECT2 and RhoA accumulation at the equatorial cortex during cytokinesis., J Cell Sci 119 (2006) 104-114.

[8] M. Glotzer, The molecular requirements for cytokinesis, Science 307 (2005) 1735-1739.

[9] U.S. Eggert, T.J. Mitchison, C.M. Field, Animal cytokinesis: from parts list to mechanisms, Annu Rev Biochem 75 (2006) 543-566.

[10] I. Mabuchi, M. Okuno, The effect of myosin antibody on the division of starfish blastomeres., J Cell Biol 74 (1977) 251-263.

[11] A. De Lozanne, J. Spudich, Disruption of the Dictyostelium myosin heavy chain gene by homologous recombination., Science 236 (1987) 1086-1091.

[12] D.A. Knecht, W.F. Loomis, Antisense RNA inactivation of myosin heavy chain gene expression in Dictyostelium discoideum., Science 236 (1987) 1081-1086.

[13] A.F. Straight, A. Cheung, J. Limouze, I. Chen, N.J. Westwood, J.R. Sellers, T.J. Mitchison, Dissecting temporal and spatial control of cytokinesis with a myosin II Inhibitor., Science 299 (2003) 1743-1747.

[14] M. Ikebe, D.J. Hartshorne, Phosphorylation of smooth muscle myosin at two distinct sites by myosin light chain kinase., J Biol Chem 260 (1985) 10027-10031.

[15] M. Ikebe, Phosphorylation of a second site for myosin light chain kinase on platelet myosin, Biochemistry 28 (1989) 8750-8755.

[16] F. Matsumura, S. Ono, Y. Yamakita, G. Totsukawa, S. Yamashiro, Specific localization of serine 19 phosphorylated myosin II during cell locomotion and mitosis of cultured cells., J Cell Biol 140 (1998) 119-129.

[17] M. Murata-Hori, N. Murai, S. Komatsu, Y. Uji, H. Hosoya, Concentration of singly phosphorylated myosin II regulatory light chain along the cleavage furrow of dividing HeLa cells, Biomed Res 19 (1998) 111-115.

[18] T. Iwasaki, M. Murata-Hori, S. Ishitobi, H. Hosoya, Diphosphorylated MRLC is required for organization of stress fibers in interphase cells and the contractile ring in dividing cells., Cell Struct Funct 26 (2001) 677-683.

[19] K. Ueda, M. Murata-Hori, M. Tatsuka, H. Hosoya, Rho-kinase contributes to diphosphorylation of myosin II regulatory light chain in nonmuscle cells., Oncogene 21 (2002) 5852-5860.

[20] S. Yamashiro, G. Totsukawa, Y. Yamakita, Y. Sasaki, P. Madaule, T. Ishizaki, S. Narumiya, F. Matsumura, Citron kinase, a Rho-dependent kinase, induces di-phosphorylation of regulatory light chain of myosin II., Mol Biol Cell 14 (2003) 1745-1756.

[21] K. Miyauchi, Y. Yamamoto, T. Kosaka, H. Hosoya, Myosin II activity is not essential for recruitment of myosin II to the furrow in dividing HeLa cells., Biochem Biophys Res Commun 350 (2006) 543-548.

[22] S. Asano, K. Hamao, H. Hosoya, Direct evidence for roles of phosphorylated regulatory light chain of myosin II in furrow ingression during cytokinesis in HeLa cells., Genes Cells 14 (2009) 555-568.

[23] T. Kondo, K. Hamao, K. Kamijo, H. Kimura, M. Morita, M. Takahashi, H. Hosoya, Enhancement of myosin II/actin turnover at the contractile ring induces slower furrowing in dividing HeLa cells., Biochem J 435 (2011) 569-576.

[24] J. Kolega, Phototoxicity and photoinactivation of blebbistatin in UV and visible light, Biochem Biophys Res Commun 320 (2004) 1020-1025.

[25] T. Sakamoto, J. Limouze, C.A. Combs, A.F. Straight, J.R. Sellers, Blebbistatin, a

myosin II inhibitor, is photoinactivated by blue light, Biochemistry 44 (2005) 584-588.

[26] K. Fumoto, T. Uchimura, T. Iwasaki, K. Ueda, H. Hosoya, Phosphorylation of myosin II regulatory light chain is necessary for migration of HeLa cells but not for localization of myosin II at the leading edge., Biochem J 370 (2003) 551-556.

[27] J. Lippincott, R. Li, Sequential assembly of myosin II, an IQGAP-like protein, and filamentous actin to a ring structure involved in budding yeast cytokinesis., J Cell Biol 140 (1998) 355-366.

[28] T. Noguchi, I. Mabuchi, Reorganization of actin cytoskeleton at the growing end of the cleavage furrow of Xenopus egg during cytokinesis., J Cell Sci 114 (2001) 401-412.

[29] F. Motegi, K. Nakano, I. Mabuchi, Molecular mechanism of myosin-II assembly at the division site in Schizosaccharomyces pombe, J Cell Sci 113 (Pt 10) (2000) 1813-1825.

[30] M. Zhou, Y.L. Wang, Distinct pathways for the early recruitment of myosin II and actin to the cytokinetic furrow, Mol Biol Cell 19 (2008) 318-326.

[31] F. Chang, A. Woollard, P. Nurse, Isolation and characterization of fission yeast mutants defective in the assembly and placement of the contractile actin ring., J Cell Sci 109 (Pt 1) (1996) 131-142.

[32] F. Chang, D. Drubin, P. Nurse, cdc12p, a protein required for cytokinesis in fission yeast, is a component of the cell division ring and interacts with profilin.,

J Cell Biol 137 (1997) 169-182.

[33] K. Oegema, M.S. Savoian, T.J. Mitchison, C.M. Field, Functional analysis of a human homologue of the Drosophila actin binding protein anillin suggests a role in cytokinesis., J Cell Biol 150 (2000) 539-552.

[34] M.P. Somma, B. Fasulo, G. Cenci, E. Cundari, M. Gatti, Molecular dissection of cytokinesis by RNA interference in Drosophila cultured cells., Mol Biol Cell 13 (2002) 2448-2460.

[35] F. Motegi, M. Mishra, M.K. Balasubramanian, I. Mabuchi, Myosin-II reorganization during mitosis is controlled temporally by its dephosphorylation and spatially by Mid1 in fission yeast., J Cell Biol 165 (2004) 685-695.

[36] T.D. Pollard, J.Q. Wu, Understanding cytokinesis: lessons from fission yeast., Nat Rev Mol Cell Biol 11 (2010) 149-155.

[37] M. Bathe, F. Chang, Cytokinesis and the contractile ring in fission yeast: towards a systems-level understanding., Trends Microbiol 18 (2010) 38-45.

[38] Y. Huang, H. Yan, M.K. Balasubramanian, Assembly of normal actomyosin rings in the absence of Mid1p and cortical nodes in fission yeast., J Cell Biol 183 (2008) 979-988.

[39] A.F. Straight, C.M. Field, T.J. Mitchison, Anillin binds nonmuscle myosin II and regulates the contractile ring., Mol Biol Cell 16 (2005) 193-201.

[40] A. Piekny, M. Glotzer, Anillin is a scaffold protein that links RhoA, actin, and myosin during cytokinesis., Curr Biol 18 (2008) 30-36.

[41] M. Kinoshita, S. Kumar, A. Mizoguchi, C. Ide, A. Kinoshita, T. Haraguchi, Y.

Hiraoka, M. Noda, Nedd5, a mammalian septin, is a novel cytoskeletal component interacting with actin-based structures., Genes Dev 11 (1997) 1535-1547.

[42] M. Kinoshita, C.M. Field, M.L. Coughlin, A.F. Straight, T.J. Mitchison, Self- and actin-templated assembly of Mammalian septins., Dev Cell 3 (2002) 791-802.

[43] E. Joo, M. Surka, W. Trimble, Mammalian SEPT2 is required for scaffolding nonmuscle myosin II and its kinases., Dev Cell 13 (2007) 677-690.

[44] Y. Oh, E. Bi, Septin structure and function in yeast and beyond., Trends Cell Biol 21 (2011) 141-148.

[45] J.G. White, G.G. Borisy, On the mechanisms of cytokinesis in animal cells., J Theor Biol 101 (1983) 289-316.

[46] D. Bray, J.G. White, Cortical flow in animal cells., Science 239 (1988) 883-888.

[47] Y.L. Wang, J.D. Silverman, L.G. Cao, Single particle tracking of surface receptor movement during cell division., J Cell Biol 127 (1994) 963-971.

[48] S. Yumura, Myosin II dynamics and cortical flow during contractile ring formation in Dictyostelium cells., J Cell Biol 154 (2001) 137-146.

[49] R.L. DeBiasio, G.M. LaRocca, P.L. Post, D.L. Taylor, Myosin II transport, organization, and phosphorylation: evidence for cortical flow/solation-contraction coupling during cytokinesis and cell locomotion., Mol Biol Cell 7 (1996) 1259-1282.

[50] S. Yumura, M. Ueda, Y. Sako, T. Kitanishi-Yumura, T. Yanagida, Multiple

mechanisms for accumulation of myosin II filaments at the equator during cytokinesis., Traffic 9 (2008) 2089-2099.

[51] T.Q. Uyeda, Y. Iwadate, N. Umeki, A. Nagasaki, S. Yumura, Stretching actin filaments within cells enhances their affinity for the myosin II motor domain., PLoS ONE 6(10) (2011) e26200.

[52] H. Miyoshi, S.K. Satoh, E. Yamada, Y. Hamaguchi, Temporal change in local forces and total force all over the surface of the sea urchin egg during cytokinesis, Cell Motil Cytoskeleton 63 (2006) 208-221.

[53] T. Kondo, R. Isoda, T. Uchimura, M. Sugiyama, K. Hamao, H. Hosoya, Diphosphorylated but not monophosphorylated myosin II regulatory light chain localizes to the midzone without its heavy chain during cytokinesis., Biochem Biophys Res Commun 417 (2012) 686–691.

[54] N.I. Naqvi, K. Eng, K.L. Gould, M.K. Balasubramanian, Evidence for F-actin-dependent and -independent mechanisms involved in assembly and stability of the medial actomyosin ring in fission yeast., EMBO J 18 (1999) 854-862.

[55] N.I. Naqvi, K.C. Wong, X. Tang, M.K. Balasubramanian, Type II myosin regulatory light chain relieves auto-inhibition of myosin-heavy-chain function., Nat Cell Biol 2 (2000) 855-858.

Figure captions

Figure 1. Characterization of MRLC-mCherry mutants

(A) Western blots of immunoprecipitates from HeLa cell lysates with Living Colors A.v. Peptide Antibody. Cells were transfected with the indicated plasmids. Myosin HC; myosin heavy chain. (B) HeLa cells expressing DD-MRLC-mCherry and EGFP-actin were fixed and counterstained with DAPI. Cells were observed by confocal microscopy. Bar, 10 μm.

Figure 2. Phosphorylated MRLC is recruited to the cell equator earlier than nonphosphorylated MRLC.

(A) HeLa cells expressing AA- or DD-MRLC-mCherry. Anaphase onset is designated as time 0. Bar, 10 μm. (B) The fluorescent intensity of AA- or DD-MRLC-mCherry at the equator (x-axis) and each accumulation time (y-axis) were plotted. (C) The average time of MRLC accumulation in cells ($n \geq 7$) expressing AA- or DD-MRLC-mCherry are indicated. $^{**}p < 0.01$ (Student's *t*-test).

Figure 3. MRLC is recruited to the cell equator earlier than actin, and the recruitment is independent of its phosphorylation state.

(A) HeLa cells coexpressing MRLC-mCherry and EGFP-actin. Anaphase onset is designated as time 0. Bar, 10 μm. (B) The fluorescent intensity of Wt-, AA-, AD-, or DD-MRLC-mCherry at the equator (x-axis) and each accumulation time (y-axis) were plotted in the cells coexpressing EGFP-actin. (C) The average accumulation time of

each MRLC mutant at the cell equator ($n \geq 6$). *$p < 0.05$ (Student's *t*-test). (D) HeLa cells coexpressing MRLC-mCherry and EGFP-actin. Anaphase onset was designated as time 0. Bar, 10 μm. (E) The fluorescent intensity of EGFP-actin at the equator (x-axis) and each accumulation time (y-axis) were plotted in the cells expressing Wt-, AA-, AD-, or DD-MRLC-mCherry. (F) The average time of mCherry-actin accumulation at the equator in cells ($n \geq 6$) expressing each MRLC mutants. (G) The average accumulation time of each mCherry-tagged MRLC mutant and EGFP-actin are shown in (C) and (F). *$p < 0.05$ (Student's *t*-test).

Figure 4. Inhibition of myosin II ATPase activity did not alter the time of actin accumulation at the cell equator.

(A) The effect of blebbistatin on the speed of furrow ingression in dividing HeLa cells ($n \geq 4$). The half-time ($t_{1/2}$) of furrow ingression is shown in the inset. *$p < 0.05$ (Student's *t*-test). (B) HeLa cells expressing mCherry-actin in the presence of DMSO (control) or blebbistatin (25 μM). Anaphase onset is designated as time 0. Bar, 10 μm. (C) Fluorescent intensity of EGFP-actin at the equator (x-axis) and each accumulation time (y-axis) were plotted in cells treated with DMSO or blebbistatin (25 μM). (D) The average time of EGFP-actin accumulation at the equator in cells ($n \geq 5$) treated with DMSO or blebbistatin (25 μM).

Figure 5. MRLC accumulation at the cell equator is independent of actin accumulation.

(A) HeLa cells treated with DMSO (control) or latrunculin A (100 nM) for 10 or 30 min were fixed and stained with TRITC-phalloidin. DNA was counterstained with DAPI. Bar, 10 μm. (B) HeLa cells expressing Wt-MRLC-mCherry in the presence of DMSO or latrunculin A (100 nM). Anaphase onset is designated as time 0. Cells treated with latrunculin A exhibited remarkable blebbing, as shown in the panel at 8 min. Bar, 10 μm. (C) Fluorescent intensity of Wt-MRLC-mCherry at the equator (x-axis) and each accumulation time (y-axis) were plotted in cells treated with DMSO or latrunculin A (100 nM). (D) The average time of Wt-MRLC-mCherry accumulation at the equator in cells ($n \geq 5$) treated with DMSO or latrunculin A (100 nM).

Figure 6. A proposed mechanism for equatorial myosin II accumulation

Before anaphase onset, phosphorylated myosin II preferentially accumulates at the cell equator (a, b). This accumulation causes an increase in cortical tension by interaction with actin, which induces a conformational change in cortical actin (c). As a result, such actin filaments enhance myosin II accumulation at the cell equator (d). Subsequently, actin accumulation or polymerization occurs (e), followed CR constriction. P-Myosin II or Non-P-Myosin II indicates myosin II binding to phosphorylated or nonphosphorylated MRLC, respectively.

Supplementary Figure Caption

Figure S1. Accumulation time of myosin II regulatory light chain (MRLC) and actin at the equator is independent of their expression levels.

The fluorescent intensity of (A) mCherry-tagged MRLC mutants or (B) enhanced green fluorescent protein (EGFP)-actin at the equator (x-axis) and each accumulation time (y-axis) were plotted in cells coexpressing MRLC-mCherry and EGFP-actin.

Figure 1

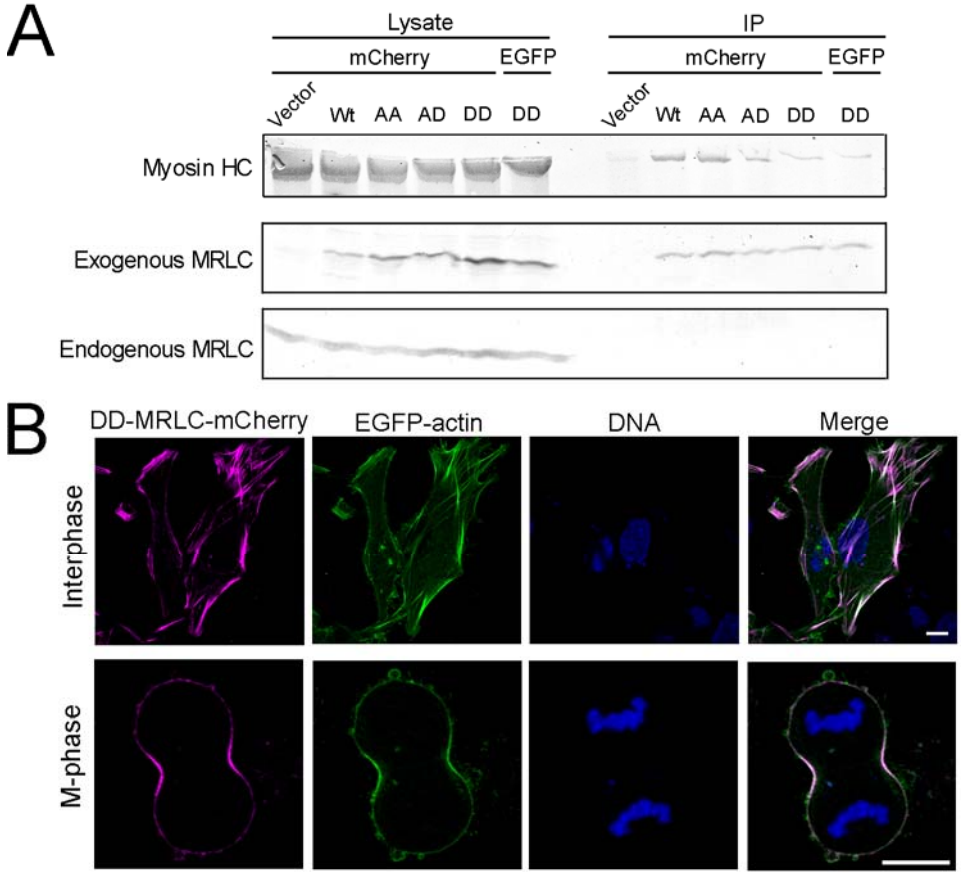
A
Lysate
IP
mCherry
EGFP
mCherry
EGFP
Vector
Wt
AA
AD
DD
DD
Vector
Wt
AA
AD
DD
DD
Myosin HC
Exogenous MRLC
Endogenous MRLC
B
DD-MRLC-mCherry
EGFP-actin
DNA
Merge
Interphase
M-phase

Figure 2

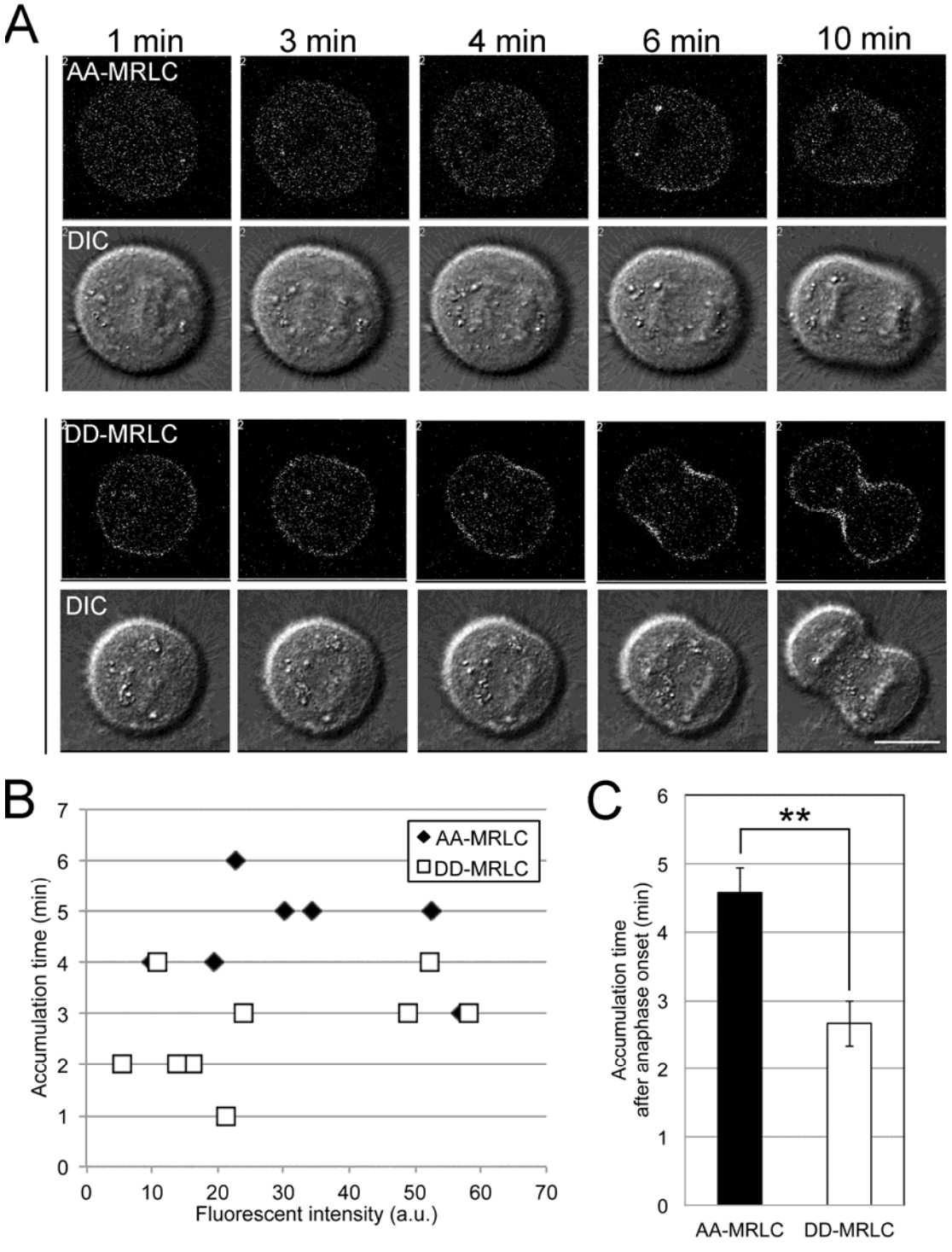
A
1 min
3 min
4 min
6 min
10 min
AA-MRLC
DIC
DD-MRLC
DIC
B
AA-MRLC
DD-MRLC
Accumulation time (min)
Fluorescent intensity (a.u.)
0
10
20
30
40
50
60
70
1
2
3
4
5
6
7
C
**
Accumulation time after anaphase onset (min)
AA-MRLC
DD-MRLC

Figure 3

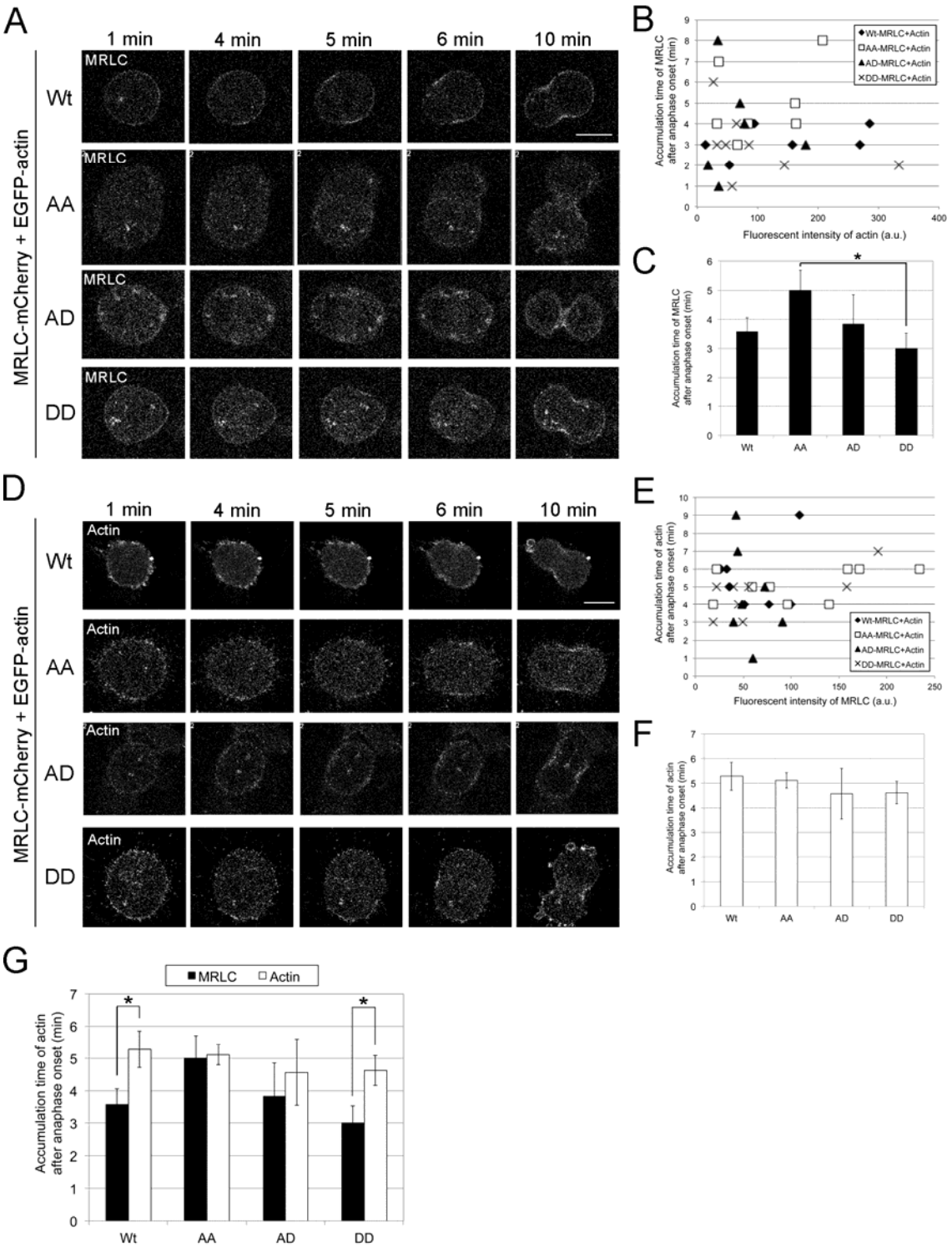
A
1 min
4 min
5 min
6 min
10 min
MRLC
Wt
AA
AD
DD
MRLC-mCherry + EGFP-actin
B
Wt-MRLC+Actin
AA-MRLC+Actin
AD-MRLC+Actin
DD-MRLC+Actin
Accumulation time of MRLC after anaphase onset (min)
Fluorescent intensity of actin (a.u.)
C
Accumulation time of MRLC after anaphase onset (min)
Wt
AA
AD
DD
D
Actin
E
Accumulation time of actin after anaphase onset (min)
Fluorescent intensity of MRLC (a.u.)
F
G
MRLC
Actin

Figure 4

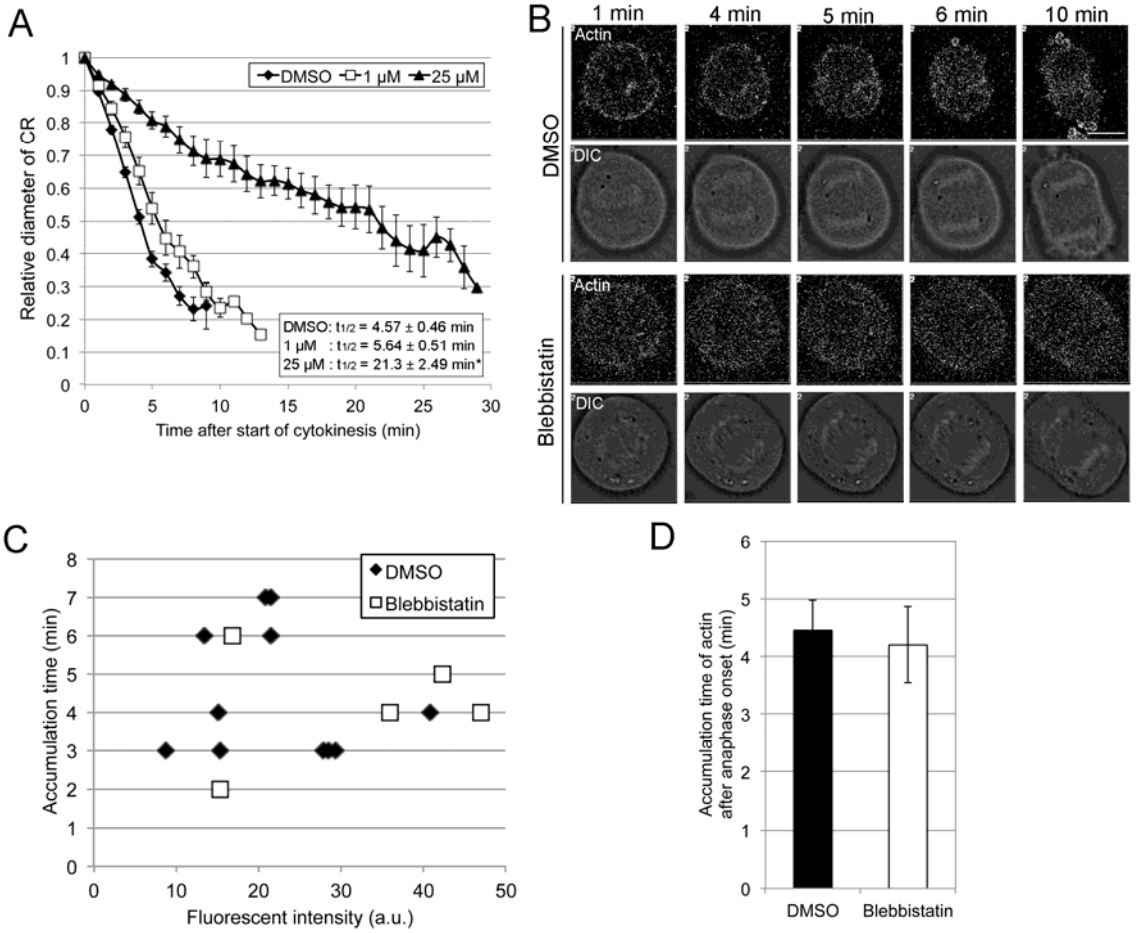
A
DMSO
1 μM
25 μM
Relative diameter of CR
Time after start of cytokinesis (min)
DMSO: t1/2 = 4.57 ± 0.46 min
1 μM : t1/2 = 5.64 ± 0.51 min
25 μM : t1/2 = 21.3 ± 2.49 min*
B
1 min
4 min
5 min
6 min
10 min
Actin
DIC
DMSO
Blebbistatin
C
DMSO
Blebbistatin
Accumulation time (min)
Fluorescent intensity (a.u.)
D
Accumulation time of actin after anaphase onset (min)
DMSO
Blebbistatin

Figure 5

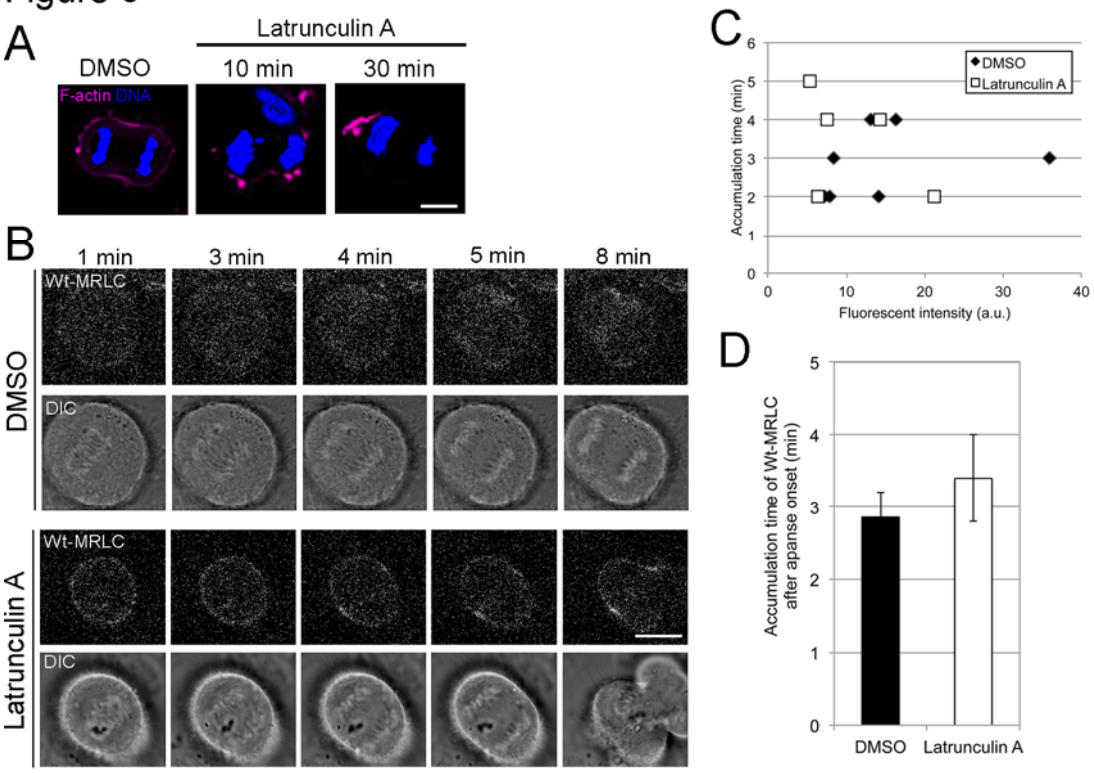
A
Latrunculin A
DMSO
10 min
30 min
F-actin DNA
B
1 min
3 min
4 min
5 min
8 min
DMSO
Wt-MRLC
DIC
Latrunculin A
Wt-MRLC
DIC
C
DMSO
Latrunculin A
Accumulation time (min)
Fluorescent intensity (a.u.)
D
Accumulation time of Wt-MRLC after apanse onset (min)
DMSO
Latrunculin A

Figure 6

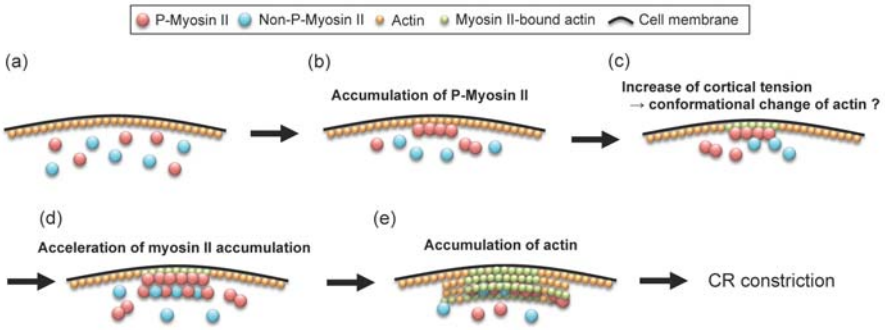
P-Myosin II
Non-P-Myosin II
Actin
Myosin II-bound actin
Cell membrane
(a)
(b)
Accumulation of P-Myosin II
(c)
Increase of cortical tension
→ conformational change of actin ?
(d)
Acceleration of myosin II accumulation
(e)
Accumulation of actin
CR constriction

Figure S1

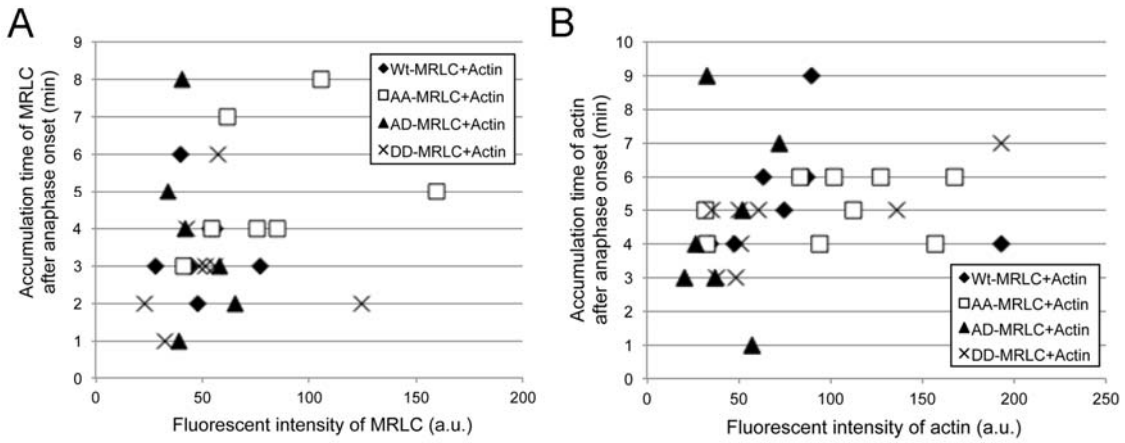
A
Accumulation time of MRLC after anaphase onset (min)
Fluorescent intensity of MRLC (a.u.)
Wt-MRLC+Actin
AA-MRLC+Actin
AD-MRLC+Actin
DD-MRLC+Actin
B
Accumulation time of actin after anaphase onset (min)
Fluorescent intensity of actin (a.u.)
Wt-MRLC+Actin
AA-MRLC+Actin
AD-MRLC+Actin
DD-MRLC+Actin